

NFCStack: Rich-ID Stacking and Interaction Based on NFC

Anonymized for review

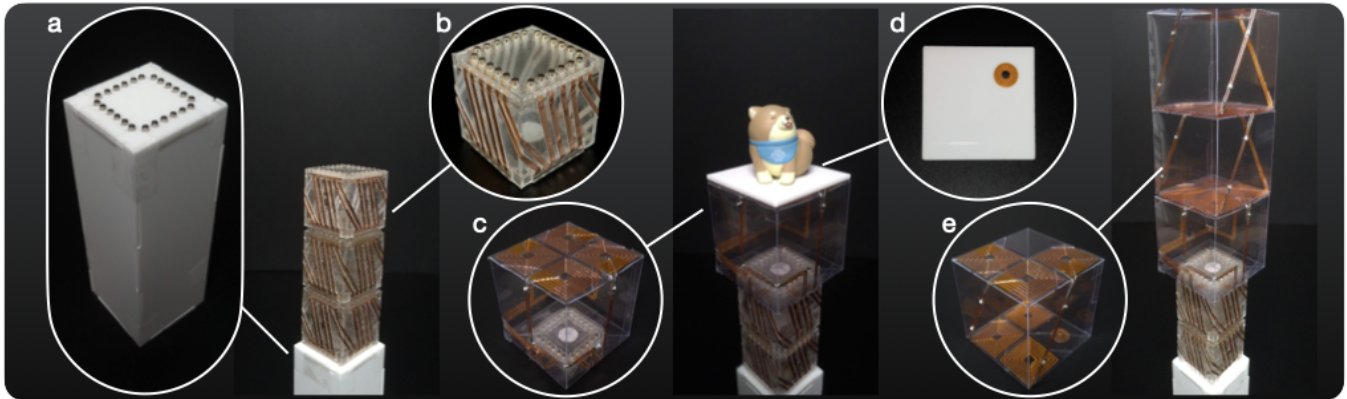


Figure 1: NFCStack is a physical building blocks system that supports rich-ID stacking and interaction. The system consists of (a) portable stations, each of them embedded a multiplexed NFC reader; (b) identifiable bricks that allow for sturdy construction; (c) identifiable adapters that turn the top of a stack into a few portals of the NFC reader, so they can detect and identify (d) an NFC-tagged token's orientation and (e) stack events of the identifiable blocks.

ABSTRACT

We present NFCStack, a physical building blocks system that supports both stacking and interaction based on near-field communication (NFC). The system consists of a portable station that can support and resolve the order of three types of passive identifiable stackables: brick, block, and adapter. The bricks support stable and sturdy physical construction, whereas the blocks support effortless tangible interactions. The adapter provides an interface between the two types of stackables and turns the top of a stack into terminals for detecting the interaction events of NFC-tagged objects. Compared with the previous systems based on NFC or radio-frequency identification (RFID) technologies, the NFCStack system is portable, supports simultaneous interactions, and resolves the stacking and interaction events responsively even when the objects are not strictly aligned. A series of evaluation results show the system effectively supports a full-stack, 12 layers of rich-ID stacking with the three types of blocks, even if every block is stacked on each other with a 6mm offset. Based on the evaluation results, we also illuminate possible generalizations such as extending this system from stacking to 2.5D construction. With our proof-of-concept implementation, we demonstrate the interaction styles through several educational application examples and discuss the design implications for future research.

KEYWORDS

NFC, building blocks, portable, tangible interaction

ACM Reference Format:

Anonymized for review. 2021. NFCStack: Rich-ID Stacking and Interaction Based on NFC. In ., ACM, New York, NY, USA, 11 pages.

1 INTRODUCTION

Stacking is one of the common abilities that we perform in a spatio-temporal organization, such as grouping or ordering things. [24]. Compare to 2D clustering, stacking is also a space-saving way to extend the property of an object while making its location perpetually stable. Therefore, HCI researchers have been seeking technological solutions to harness stacking as a form of tangible interface [14] to leverage our existing cognitive and spatial knowledge to comprehend the embodied digital information.

Passive radio-frequency identification (RFID) or near-field communication (NFC) technologies have been recently considered by HCI researchers because they have virtually infinite ID space, are less affected by the line-of-sight problem, and support straightforward maintenance. Although RFID does not primitively support the resolution of tagged object stacking, researchers have proposed using contact switches [13] or using collision avoidance mechanism [35] to resolve the order of stacking of RFID-tagged objects from the sequential stack events. However, it is still challenging for these systems to resolve concurrent stack events simultaneously happening from multiple input sources.

In this paper, we present NFCStack (Figure 1), a physical building blocks system that supports both stacking and interaction based on near-field communication (NFC). Our solution to the challenge is the proposed extendable antenna design that allows a multiplexed

Permission to make digital or hard copies of part or all of this work for personal or classroom use is granted without fee provided that copies are not made or distributed for profit or commercial advantage and that copies bear this notice and the full citation on the first page. Copyrights for third-party components of this work must be honored. For all other uses, contact the owner/author(s).

UIST '22,

© 2021 Copyright held by the owner/author(s).

117 NFC reader to track the stack event at every height through a different channel, so concurrent actions can be resolved. Also, robust
 118 and responsive stack tracking can be achieved.
 119

120 To support both rich-ID stacking and tangible interaction, the
 121 system provides three types of passive identifiable stackables: brick,
 122 block, and adapter. The bricks are interconnected by magnetic
 123 connectors, which support sturdy stable physical construction. In con-
 124 trast, the blocks support effortless tangible interaction, because they
 125 are wirelessly inter-connected using conductor coils. The adapter
 126 provides an interface between the two types of stackables and turns
 127 the top of a stack into terminals for detecting the interaction events
 128 on the top of it, such as an NFC-tagged token's orientation or stack
 129 events of the identifiable blocks.

130 With our proof-of-concept implementation, we evaluated the
 131 system's capability. A series of evaluation results show the sys-
 132 tem effectively supports a full-stack, 12-layers of rich-ID stacking
 133 with the three types of blocks, even if every block is stacked on
 134 each other with a 6mm offset. Based on the evaluation results, we
 135 also illuminate possible generalizations such as extending this sys-
 136 tem from stacking to 2.5D construction. We also demonstrate the
 137 enabled interaction styles through several applications examples.

138 The main contribution of this work is the engineering and design
 139 of a physical building blocks system that is capable of resolving
 140 concurrent stacking and blends two additional input modes into
 141 the conventional NFC interaction.

142 In the following sections, we first discuss the related work. Then,
 143 we present the design, implementation, and evaluation of our proof-
 144 of-concept implementation. Last, we discuss the design implications
 145 and future research directions with preliminary results.

147 2 RELATED WORK

148 2.1 Constructive Assembly and Stackables

149 Constructive assemblies of modular, interconnecting elements fa-
 150 cilitate physical modeling and geometrical representations, such as
 151 Lego bricks¹ and Mecanno². Applying constructive assemblies in
 152 HCI as a tangible user interface [14, 34] can afford reality-based in-
 153 teractions that leverage the users' body, social, and environmental
 154 awareness, and skills, as well as their common senses the Euclidean
 155 physics [15]. The rich embodied and kinetic experiences can be
 156 useful, especially in learning abstract concepts [36] or exploring de-
 157 sign opportunities, which has been demonstrated in many previous
 158 work [29, 31].

159 Stacking brings the building blocks into the third dimension.
 160 Researchers have applied embedded electronic circuits and sensors,
 161 such as motion sensors [12], IR sensor array [2], and conductive
 162 dot patterns [9] to detect the stack events. Nonetheless, these power
 163 electronics require deployment and maintenance costs that are
 164 significant when they are deployed at scale. Researchers also applied
 165 passive sensing techniques such as optical markers [5], markered
 166 fiber-optic bundle [6], capacitive footprints [7], pressure image [18],
 167 magnetic-field image [19, 22] to allow its state of stacking to be
 168 detected by an external sensor. However, the ID space and stacking
 169 height are limited in these solutions.

170 ¹<http://www.lego.com>

171 ²www.meccano.com

172 2.2 Identifiable building blocks

173 Identifiable building blocks can support the semantic construction
 174 of information. Previous works make identifiable building blocks
 175 with embedded micro-controllers and/or power-line communica-
 176 tion protocols (e.g., I^2C) to identify the building blocks that are used
 177 for semantic construction in the built geometry [1, 10, 16, 17, 27, 30].
 178 Additionally, they offer extra interactivity with the sensors and the
 179 actuators connected to them. Nonetheless, reducing their electromechanical
 180 interconnections is not always straightforward, so they
 181 usually support only fixed, rigid constructions and cannot reli-
 182 ably detect objects that are not strictly aligned. Moreover, these
 183 electronic elements also require additional hardware costs and
 184 maintenance that are significant when they are deployed at scale.

185 Passive RFID building blocks support straightforward mainte-
 186 nances when they are deployed at scale. RFIBricks [13] is a rich-ID
 187 building blocks system based on modified ultra-high-frequency
 188 (UHF) RFID tags. RFIBricks harnessed the near-field effects of a far-
 189 field UHF RFID system by allowing a unique pair of normally-off
 190 tags to be turned on simultaneously while stacking. As a result, the
 191 system provides a volumetric interaction stage where the build-
 192 ing block units stay passive. RFIBricks system also requires and
 193 facilitates strict alignment between the building blocks by using
 194 magnetic connectors, which makes the (un)stacking operations
 195 effortful. Although a follow-up work RFIMatch [21], demonstrates
 196 that such a correlated state change can be achieved without physical
 197 contact by incorporating a magnet-biased reed switch mechanism,
 198 how to implement such a mechanism in a building blocks system
 199 is still unknown.

200 The most fundamental limitation of the UHF RFID approach is
 201 that the interaction area is defined by the antenna connected to the
 202 bulky, power-consuming, and expensive UHF reader. The building
 203 blocks also cannot be effectively miniaturized due to the tag-to-tag
 204 interference in a high-density tag deployment. Last but not least,
 205 it does not support concurrent events, which frequently occur in
 206 multi-user or bimanual interactions with smaller objects.

207 Previous work also explored the design space of passive rich-
 208 ID building blocks with NFC. Project Zanzibar [35] also explored
 209 rich-ID stacking with NFC by using a relay coil structure, namely
 210 Stacker, to extend the power and data transfer from the mat of
 211 the NFC antenna matrix to the upper layers of the stack. When
 212 a user sequentially stacks one on the other, the new tags can be
 213 activated and read with the dynamic frame slotted aloha (DFSA) [8]
 214 collision avoidance mechanism. Like RFIBricks, Zanzibar also does
 215 not support concurrent events because the appearance order of
 216 simultaneous multi-tag appearances cannot be guaranteed in NFC.
 217 Furthermore, the response time linearly increases with the layer
 218 number of the stack by the nature of the DFSA algorithm, down-
 219 grading the reliability and the user experiences when the stack goes
 220 higher. The delays in such makes the common stack operations
 221 (e.g., re-ordering) inefficient and unreliable.

222 2.3 Tangible Interaction with NFC

223 NFC systems or high-frequency RFID systems (HF RFID) have
 224 been broadly applied in tangible interaction for identifying passive
 225 tagged objects [4, 25, 32]. Compared with other sensing technolo-
 226 gies based on electromagnetic induction such as [28, 33], NFC/RFID

systems are off-the-shelf and very easy to use for prototyping. The near-field sensing range allows interaction can be contactless and therefore effortless. In addition to the popular toys-to-life applications, such as Nintendo Amiibo³ and Lego Dimensions⁴, researchers have also used commodity off-the-shelf NFC tags for sensing user inputs such as detecting speed and frequency [20] and used multiple tags as a compound widget [3, 11, 20]. In this paper, we also aim at supporting effortless tangible interactions with the NFCStack system.

3 ANTENNA EXTENSION METHODS

To identify an NFC-tagged block stacked on top of a stack of blocks on the station, the blocks shall extend the detection range of the underlying reader's antenna to the top surface. We first explain the theoretical background and then introduce the two antenna coil extension methods that we considered and explored: 1) transmission lines extension and 2) multi-hop extension.

3.1 Background

NFC readers and tags operate at $f = 13.56\text{MHz}$. To build wireless antennas that harness the power and signal of NFC readers and tags, an RFC resonant circuit is needed, where R , L , and C stand for resistor, inductor, and capacitor, respectively.

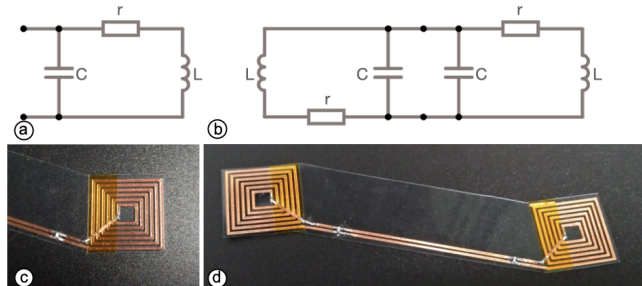


Figure 2: Half relay and full relay: Schematics of (a) a half relay and (b) a full relay; realization of (c) an half relay and (d) a full relay.

Figure 3a portrays the schematic of a typical RLC circuit, we call it a *half relay* in this paper. A proper R , L , and C has to be chosen to satisfy two conditions: 1) $f_0 = \frac{1}{2\pi} \sqrt{\frac{1}{LC} - (\frac{R}{L})^2} \sim f$, where f_0 is the resonant frequency of the RLC circuit, and 2) $Q = \frac{1}{R} \sqrt{\frac{L}{C}}$, $30 \geq Q > 1$ where Q is the quality factor of the RLC circuit. $Q = 30$ is the theoretical upperbound for ensuring a sufficient bandwidth for full-speed (424kbit) near-field communication. When the two condition are satisfied, the RLC circuit can effectively and efficiently resonate at the frequency $f_0 \sim f$.

Figure 3a portrays the schematic of a full relay, which consists of two half relays connected by the transmission lines, which is a pair of parallel conducting wires. One conductor coil receives the NFC signal based on magnetic induction and then relays the signal through the transmission lines to the other conductor coil. When a

³<https://www.nintendo.com/amiibo>

⁴<https://www.lego.com/en-us/dimensions/products>

pair of conductor coils from different relays are sufficiently coupled in proximity, the power and signals can be wirelessly transferred from one to another.

Nonetheless, when one conductor coil is coupling with another one at a distance, the geometric dimensions of two conductors coils has an effect on the two coils' power transfer efficiency. For instance, assuming two conductor loop coils L_a and L_b has an radius of r_a and r_b , respectively, the coupling coefficient k is formulated as:

$$k(x) = \frac{r_a^2 \cdot r_b^2}{\sqrt{r_a \cdot r_b \cdot [\sqrt{x^2 + max(r_a, r_b)^2}]^3}} \quad (1)$$

where x is the lateral distance between L_a and L_b . $k = 1$ can be achieved where $x = 0$ and $r_a = r_b$. In practice, however, inductively coupled transponder systems operate with coupling coefficients that may be as low as $k = 0.01$ ($< 1\%$) [8]. Still, to make the coil withstands an offset x' , it is preferred to use similar size and large-enough coil (e.g., $r_a \sim r_b \gg x'$) for both conductor coils.

3.2 Transmission Lines Extension

The conductor coil's location can be mechanically extended from the reader with a pair of parallel transmission lines, as shown in Figure 3a. With low-ohmic electromechanical connectors, multiple segments of transmission lines can be connected to extend the transmission line further. A physical part can be identified with an NFC-tagged coil, which has two terminals that can be connected to a pair of transmission lines.

The simple method only requires small footprints, making it a good candidate for making small building blocks. However, this method also requires a firm low-ohmic electromechanical connection that may impede the HCI, because a reliable connection requires more physical efforts to pull two parts apart. Relaxing the alignment constraint between two parts without compromising the low-ohmic connection is challenging if not impossible. Last but not least, the additional capacitance that is proportional to the length of transmission lines may affect the tuning of the RLC circuits.

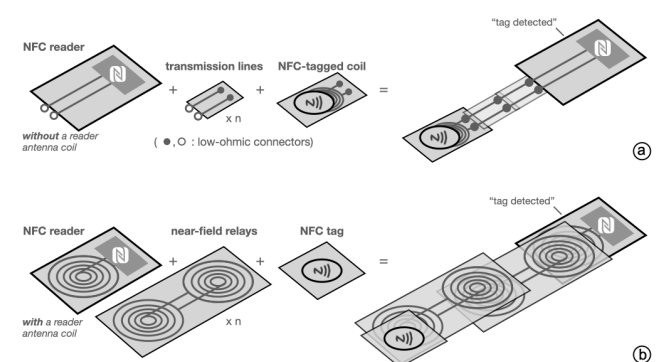


Figure 3: Two antenna extension methods; (a) transmission lines extension; (b) multi-hop extension.

3.3 Multi-Hop Extension

To afford *effort-less* interactions, the conductor coils' location can be extended by multiple hops of relay connections, as shown in

Figure 3b. Therefore, without any electro-mechanical connectors or physical contact, a multi-hop connection can be realized with multiple relays segments. The coil at the end of these chained relays serves as an NFC reader that can detect an NFC tag in its near field.

Figures 3c and d show example half relay and full relay implementations with 2cm-width rectangular conductor coils that supports multi-hop extension. They can effectively transmit powers to each other with a sub-centimeter offset, but they also require a larger footprint than the transmission lines extension. When the length of transmission lines is short, the additional transmission lines' capacitance is negligible so it does not affect the RLC antenna tuning.

3.4 Summary

Both methods extend the conductor coil from NFC readers to another location. Each of them also provides advantages depending on different purposes of use. When the main purpose is constructing physical form, the transmission lines extension method provides more rigidity in the construction and allows each physical unit to be made smaller. On the other hand, when the main purpose is tangible interaction, the multi-hop extension method supports a more versatile set of effortless tangible interactions. Therefore, it is suitable to use the blocks made of transmission lines for supporting study construction and to use the blocks made of near-field relays for building interactive elements in the system.

Constructive assembly tangible UI systems need both constructive and interactive elements. Therefore, a system that is compatible with both types of building blocks is desirable. In the later section, we present a proof-of-concept realization of such a system.

4 SYSTEM DESIGN AND IMPLEMENTATION

Based on the aforementioned methods, we present the design of three types of building blocks and one *station* that can resolve the stacking order of all these blocks. Proof-of-concept implementations are presented as a realization of the design and used for showcasing the interaction techniques. Implementation details are presented thereafter.

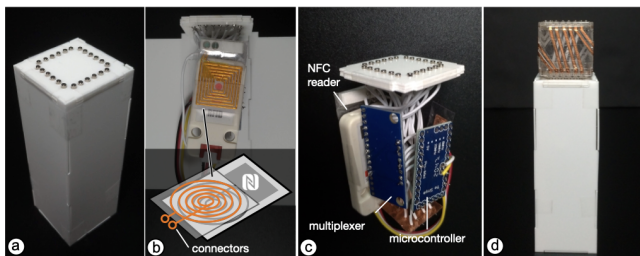


Figure 4: Station: (a) overview; (b) half-relay extension from the NFC reader antenna; (c) signal processing unit; a brick stacking on the station.

4.1 Station

To support concurrent stack events and more robust and extensible stack sensing, each layer of stacking has to be detected individually.

Therefore, the station applies a multiplexed NFC reader to enable the resolution.

Figure 4 shows the station design with an example implementation. Each station's top surface is the same as the block's top surface, so it also has M pairs of two magnetic connectors ($T_{top}^i = \{T_{in}^i, T_{out}^i\}$, where $1 \leq i \leq M$) as its terminals on its top surface. T_{in}^i is the input connector of the terminal T_{top}^i , and T_{out}^i is the output connector of the terminal T_{top}^i . To detect all the NFC tags of multiple blocks stacked on the station, the station consists of an NFC reader connected to a multiplexer circuitry via the reader's two antenna terminals, A_{in} and A_{out} , which were supposed to connect an external half-relay. The A_{in} is connected to the input of a 1-to- N multiplexer, of which M out of the N output channels are connected to the T_{in}^i . The remaining T_{out}^i are connected to the A_{out} .

4.2 Building Blocks

The three types of building blocks are *brick*, *block*, and *adaptor*.

4.2.1 Brick. A brick (Figure 5) is an identifiable stackable unit based on the transmission line method. Each brick consists of M pairs of two magnetic connectors as its terminals T on its top (T_{top}^i) and the bottom (T_{bottom}^i) surfaces, where $1 \leq i \leq M$. $M - 1$ pairs of transmission lines t_j are connected between (T_{top}^j) and (T_{bottom}^{j+1}), where $1 \leq j \leq M - 1$. Terminal T_{bottom}^1 is connected to a coil at the center of the block's bottom surface through a pair of transmission lines; on the other hand, the terminal T_{top}^M is not connected to any coil. An NFC tag is attached close to the conductor coil of a half-relay so that the tag can be detected by the coil through the relay when it is connected to the reader, as shown in Figure 4d. A brick stacking at the n th-layer can be detected by the station's terminal T_{top}^n (through the terminal T_{top}^1 of the $n - 1$ -layer block) under it.

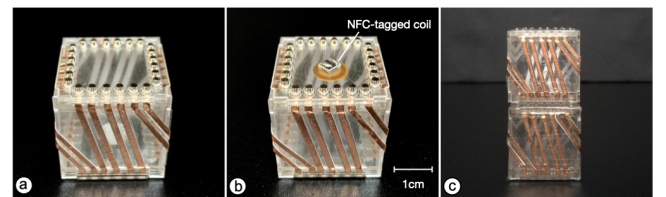


Figure 5: Bricks: (a) top view; (b) bottom view; (c) a brick stacking on another brick.

4.2.2 Block. A block (Figure 6) is an identifiable stackable unit based on the near-field relay method, so it does not require any electro-mechanical connection (i.e., the magnetic connectors). Similar to the brick design, each block consists of N terminals. One terminal T on its top (T_{top}^i) and another one is on the bottom (T_{bottom}^i) surfaces, where $1 \leq i \leq N$. $N - 1$ relay r_j are used to connect (T_{top}^j) and (T_{bottom}^{j+1}), where $1 \leq j \leq N - 1$. An NFC tag is attached to the location of T_{bottom}^1 , so a block stacking at the n th-layer can be detected by the station's terminal T_{top}^n (through the T_{top}^1 conductor coil of the $n - 1$ -layer block) under it.

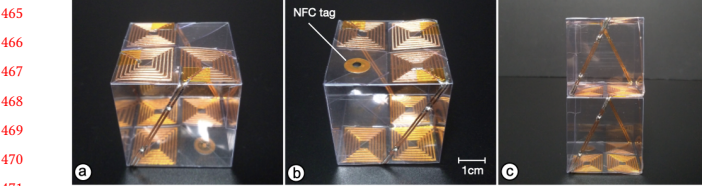


Figure 6: Block: (a) top view; (b) bottom view; (c) a block stacking on another block.

4.2.3 *Adapter*. An adapter (Figure 7) is an identifiable stackable unit for bridging a brick and a block, so the bottom side of it is similar to the brick and the top side of it is similar to the block. For an N -way adapter, the bottom of an adapter consists of $N+1$ pairs of two magnetic connectors as its terminals T on its bottom (T_{bottom}^i) surfaces, where $1 \leq i \leq N+1$. Terminal T_{bottom}^1 is connected to a conductor coil at the center of the block's bottom surface through a pair of transmission lines. An NFC tag is attached close to the coil so that the tag can be detected by the coil when the antenna is connected to the reader. The rest of each terminal T_{bottom}^i , where $2 \leq i \leq N+1$, is connected to the half-relay at $T_{top}^{(i-1)}$.

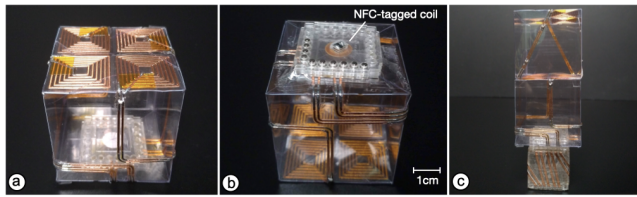


Figure 7: Adapter: (a) top view; (b) bottom view; (c) an adapter interfacing a brick and a block.

4.3 Stacking Building Blocks on Stations

Bricks for Construction. Bricks are suitable for building stable structures that can sustain the state even when the station is held in hand. Figure 8a shows a stack of $M = 12$ -terminal bricks stacked in the same direction. The antenna circuitry aggregates signals from the top of all layers of blocks to the different channels of the multiplexer in the station. Alignment between every two blocks is guaranteed by the magnetic connectors, which are applied on the top and the bottom of the brick as well as the top of the station. As a result, the identity of each brick can be picked up by the reader antenna, and its stacking layer height h is resolved by knowing which multiplexer channel i detects the tag, where $1 \leq i \leq M$. In this case, the ideal maximum height of stacking is $h_{max} = M$.

Figure 8b shows a stack of brick stacked with a rotation. The orientation θ and stack height h of each block can be resolved as $\theta = \frac{\pi}{2} \lfloor i/4 \rfloor$ and $h = (i \bmod 4) + 1$, respectively, when the multiplexer's channel i detected the tag. In this case, the ideal maximum height of stacking is $h_{max} = M/4$.

Adapter. Adapter that turns the top of the stack into multiple terminals that can read NFC tags. When the N -way adapter is stacked on the i layer, the identity of each identity can be picked up by the

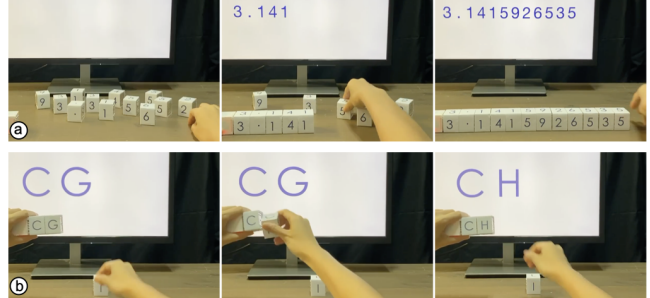


Figure 8: Stacking bricks on a station: (a) without rotation; (b) with rotation.

reader antenna through the multiplexer channel i . Furthermore, the N terminals on the top, T_{top}^j , where $1 \leq j \leq N$, serves as an extension of the next N multiplexer channel $i+j$ to detect and identify an NFC tag in its near field, as long as $i+j \leq M$, where M is the number of the station's terminals. Figure 9 shows the application of an adapter on a station or a stack of bricks stacked on the station, which can be used for reading N NFC tags.

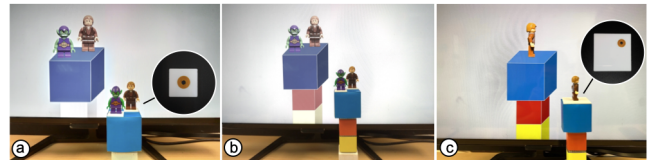


Figure 9: Adapter that turns the top of stack into multiple NFC readers: (a) stacking an adapter on the station for sensing other NFC tags; (b) adding directly on a stack of bricks; sensing the orientation of a tagged token.

Blocks for Interaction. Blocks are suitable for building interactive elements on the adapter because they afford effortless operations. Figure 10b shows a stack of $N = 4$ -terminal blocks stacked in the same direction on a N -way adapter. Similar to bricks, the identity of each brick can be picked up by the reader antenna through the terminal of the adapter, and its stacking layer height h is resolved by knowing which multiplexer channel i detects the tag, where $1 \leq i \leq M$. Nonetheless, the ideal maximum height of block stacking is the terminal numbers N of the N -way adapter.

Figure 10c shows a block stacked on an adapter with a rotation. The orientation θ and stack height h of each block can be resolved as $\theta = \frac{\pi}{2} \lfloor j/4 \rfloor$ and $h = (j \bmod 4) + 1$, respectively, when the adapter's terminal j detected the tag. In this case, the ideal maximum height of stacking is $h_{max} = N/4$.

Figure 10a shows the application of reading N NFC tags on the top of the stack when the maximum stack height h_{max} is not reached. Even if the maximum height is reached, new NFC tags can still be read if the reader supports the ISO 15693 collision-avoidance mechanism.



Figure 10: Stacking blocks on the adapter stacked on the station: (a) sensing other NFC tags; (b) without rotation; (c) with rotation.

4.4 Application Examples

We present two simple use cases to exemplify how these three types of blocks can be featured in applications.

Q & A. Figure 10 shows a word puzzle game. Several letter bricks and letter blocks are provided for the users. One user (i.e., the questioner) stacks a sequence of bricks on one side and adds an adapter to the end to set the puzzle. And another user (i.e., the student) tries to guess the sequence of blocks on the other side by trying out with the blocks, which he can easily switch. When a correct brick is in the correct position, the display shows the character as the feedback. When the student needs a hint, he uses an NFC token to show the next character on the screen, but the hint works only once for each quiz. Then, the student uses the rest of the blocks to finish the answer.

Interactive Music Sequencer. Figure 11 shows an interactive music sequencer, where several music note bricks, two adapters, and several instrument blocks are provided for the users. The users first stack a sequence of notes on the station and put an adapter on the stack to finalize it. Then, the users stack the instrument block, which has one instrument on each of the four faces, on the adapter and the note sequence starts looping with the selected instrument. The users change the instrument that will be used in the next loop by rotating the block. If they have built a second track with another station, they can stack another instrument on the second stack to make a chorus. The timing of both tracks is synchronized.

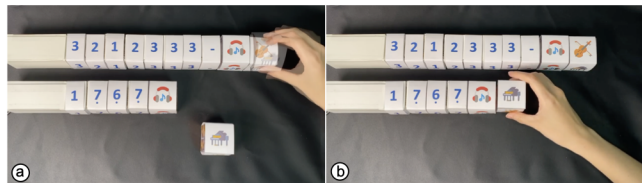


Figure 11: Interactive Music Sequencer: (a) selecting the instrument on the first track by rotating the block; (b) selecting the instrument for the second track.

4.5 Implementation

Station. Each $M = 12$ station has a dimension of $30 \times 30 \times 100$ mm 3 , supporting a maximum of 12 layers of stacking. An RC522 NFC reader is used in each station. Without modifying the original hardware, we apply a thin copper-foil half relay on top of the NFC reader's antenna so we can obtain the NFC signal

from the two terminals, as shown in Figure 4b. To achieve a high coupling coefficient k , we align the coil to the center of the reader's antenna coil, and make the half relay's conductor coil dimensions similar to the reader's antenna coil. The half relay has a 6-turn 20 mm (ϕ) \times 0.1 mm (T) 0.47 uH conductor coil wined by 0.8 mm width of vinyl-cut copper trace with a 0.6 mm gap distance between trace, and a 300 pF surface mounted parallel capacitor to tune its resonant frequency $f_0 \sim 13.56\text{MHz}$.

The top surface of a station is the same as the brick's top surface. It has twelve pairs of two magnetic connectors. The time-domain multiplexed NFC reader circuitry is built with a commodity off-the-shelf MFRC522 NFC reader, a 1-to-16 TI CD74HC4067 multiplexer, and an Arduino Pro Mini board. The tag events are captured by the microcontroller and then sent to the application through a serial connection. The NFC reader's read rate was set to 250 reads per second (rps), so each of the 16 terminals has an interactive read rate of ~ 15.6 rps.

Building Blocks. Regarding the physical structures. The bricks and stations are made with laser-cut acrylic sheets of 1mm thickness, while the adapters and blocks are made of 0.25mm-thick vinyl-cut polythene sheets.

Brick. Each $M = 12$ brick has a dimension of $30 \times 30 \times 30$ mm 3 . For each of the brick, twelve pairs of two magnetic connectors, are deployed on both top and the bottom of the block, three pairs per side. The magnetic connectors are convex N35 neodymium magnets whose size at the bottom was 3 mm (ϕ) \times 1 mm (T) and, at the top, 2 mm (ϕ) \times 2 mm (T). To extend the NFC read range, eleven pairs of two transmission lines made of 2 mm (W) copper tape with a 1.4mm gap distance are deployed on each brick to connect the magnetic connectors. To provide its identity, an off-the-shelf 4.5 mm (diameter; ϕ) \times 3.2 mm (thickness; T) 1.4 uH Bourn SDR0403-1R4ML unshielded inductor is attached to the bottom of the brick with a 10 mm (ϕ) NTAG213 NFC tag attached to it. Using such small inductors for the bricks its fine because the physical alignment is guaranteed by the magnetic connectors.

Block. Each $N = 4$ block has a dimension of $45 \times 45 \times 45$ mm 3 , which is almost twice larger than the bricks. $N - 1 = 3$ vinyl cut relays are deployed on the block. Each relay is made of two 6-turn 20 mm (ϕ) \times 0.1 mm (T) 0.47 uH coils wined by 0.8 mm width of vinyl-cut copper trace with a 0.6 mm gap distance between trace, a 300 pF surface mounted parallel capacitor, and a pair of transmission lines made of copper tape in 0.8 mm trace width and 0.5 mm gap distance. To provide its identity, a 10 mm (ϕ) NTAG213 NFC tag is attached to the location T_{bottom}^M .

Adapter. Each $N = 4$ -way adapter has the same top surface configuration as the block and the same bottom surface configuration as the brick. A laser-cut magnetic adapters used in the brick is attached to the bottom. The adapter has a height of 45 mm.

5 SYSTEM EVALUATION

5.1 Performance of Antenna Extension

The first study investigates the extendable antenna's performance after stacking.

Apparatus. A NanoVNA v2 vector network analyzer (VNA) and standard $50\ \Omega$ SMA connectors were used for measurement (Figure 12). Twelve blocks and twelve relays, which are the same as what we used in the blocks, were used in the test. For measuring the bricks, channel 1 of the VNA was connected to the bricks through a pair of magnetic connectors. For measuring the relays, a coil extender, which is in the same specification as what we used in the stations, was connected to channel 1 of the VNA. An NFC tag, which is the same model as what we used in the building blocks, was connected to channel 2 of the VNA.

Procedure. Each measurement was taken after a block was stacked on the station. We connected the antenna's terminals to the port of the VNA via the SMA connector and measured its S11 return loss and S21 power between 10.92MHz and 16.2MHz. We took the sweep of 5 measurements, discarded two outlying samples, and averaged the rest of the three as a result. Twelve results were collected from 1 to 12 layers of block/brick stacking.

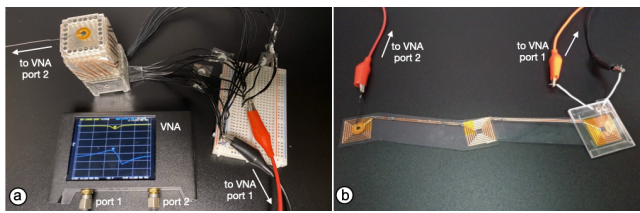


Figure 12: Experimental apparatus for evaluating the performance of antenna extension: (a) example settings for S11 measurement (with a brick and a tagged coil; layer 2); (b) example settings for S21 measurement (with two relays and a tag; layer 3).

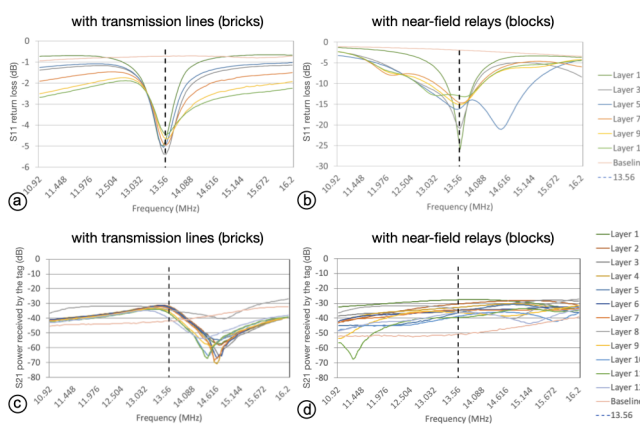


Figure 13: Antenna extension performance: (a) S11 measurement of transmission lines extension; (b) S11 measurement of multi-hop extension; (c) S21 measurement of transmission lines extension; (d) S21 measurement of multi-hop extension.

Results. Figure 13 shows the S11 and S21 measurement results. Only the results of odd-number layers of stacking are visualized for clarity of visualization. The S11 measurement results represent the reflected power that the VNA tried to deliver to the antenna through port 1. The results show both methods achieved the impedance match between the power source and the inductor at 13.56 MHz regardless of the height of brick stacking or the number of relay connections. This signifies that our implementation of both methods is effective. Nonetheless, it is observable that the S11 return loss of using the multi-hop extension is higher than that of using the transmission lines extension, showing that more power was either radiated or absorbed as losses within the antenna.

Therefore, we also check the S21 measurement, which represents the power transferred from Port 1 to Port 2, to see whether the tag receives sufficient power. The result shows that the NFC tag also received sufficient energy at 13.56 MHz regardless of the height of brick stacking or the number of relay connections. Except for the twelfth layer of the bricks, all other measurements received clearly higher power than the baseline condition that the tag does not receive any signal. Therefore, we conclude that our implementations of the two antenna extension methods are effective.

5.2 Performance of Stacking

The second study investigates the systems stack sensing capability. Three sessions of measurements were conducted.

5.2.1 Session 1: Full Stack on One Station.

Apparatus. Twelve bricks, one adapter, four blocks, and one station were used for the measurement.

Procedure. First, we randomly chose one brick from the pool of blocks to stack on the station and took 3-second, 45 reads of every NFC tag on the station. Suppose $> 95\% = 43$ reads of all the tags on the two stations were successful. In that case, we stack another layer of brick/adapter/block to the station and take other 3-second reads until the reads do not meet the success criteria, or reach the 12-layer height limit. Two extreme conditions were tested: 1) a stack of 12 bricks, and 2) a stack of a sequence of 7 bricks, 1 adapter, and 4 blocks. Five iterations were taken for the measurement.

Results. The station passed the full-stack test in all five iterations under these two extreme conditions, showing that the system is able to reliably handle the stacking of all three types of building blocks in a single station setting.

5.2.2 Session 2: Offsets Between Blocks vs. Block Stacking. The second study investigates how the blocks' stacking performance is affected by the misalignment between the blocks. As discussed in Section 3.1, the offsets between the coils that decrease the coupling factor affect the power transfer efficiency.

Apparatus. Similar to session 1, twelve bricks, one adapter, four blocks, and one station was used for the measurement, but only the four blocks are used for testing. A few 2mm-thick acrylic sheets were used as spacers to maintain the offset distances between two blocks, as shown in Figure 14a.

Procedure. We first set up two initial conditions: 1) a stack of only 1 adapter, which represents the easiest condition, and 2) a stack of a

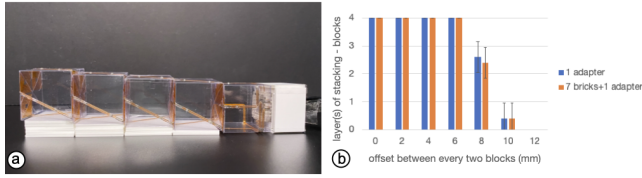


Figure 14: Offsets between blocks vs. block stacking: (a) experiment apparatus ($x = 4\text{mm}$); (b) results.

sequence of 7 bricks, 1 adapter, which represents the most difficult condition. Under each condition, we take the same procedures as Session 1. Each layer of one block was added to the stations with an $x\text{-mm}$ offset against the block or adapter in the previous layer and take a 3-second read until the reads do not meet the success criteria or the 4-layer height limit is reached. 7 distances between $d_{\text{station}} = 0$ to 12 mm (2mm step) were measured. Five iterations were taken for each offset.

Results. Figure 14b shows the results. The station passed the full-stack test in all five iterations under these two extreme conditions when $x \leq 6\text{mm}$, showing that the system is able to reliably handle the stacking of blocks with a slight offset. Also, even when the stack can only resolve $M=2.6$ layers (SD) and $M=2.4$ layers (SD) in conditions 1 and 2 respectively when $x = 8\text{mm}$, it was already difficult to stack these blocks vertically for more than two layers without letting them collapses. Therefore, we believe the current system is sufficient to support basic usage and withstand effortless stacking.

5.2.3 Session 3: Station Distance vs. Brick Stacking. The third study investigates how the brick stacking performance is affected by the distance between the two stations because the small proximity between the neighboring transmission lines potentially affects the NFC sensing performance.

Apparatus. Twenty-four and two stations were used for the measurement. Blocks and adapters were not used here because they are larger than the station. A few 1mm-thick acrylic sheets were used as spacers to maintain the distance between the stacks, as shown in Figure 15a.

Procedure. The procedure is similar to session 1. Each layer of two blocks was added to the stations and take 3-second reads until the reads do not meet the success criteria or the 12-layer height limit is reached. 7 distances between $d_{\text{station}} = 0$ to 6 mm (1mm step) were measured. Five iterations were taken for each distance.

Results. Figure 15b shows the results. The brick's stack height increases from $M = 3.6$ (SD = 0.55) at $d_{\text{station}} = 0\text{mm}$ to $M = 11.6$ (SD = 0.55) layers at $d_{\text{station}} = 5\text{mm}$ and $d_{\text{station}} = 6\text{mm}$. Although the two stations did not pass the full stack test in two out of the five iterations when $d_{\text{station}} = 5\text{mm}$ and $d_{\text{station}} = 6\text{mm}$, they achieved at least 11 layers of reliable brick stacking in all the iterations.

6 GENERALIZATIONS OF NFCSTACK

Based on the experiment results, we further developed a 2.5D construction as a generalization of the NFCStack system.

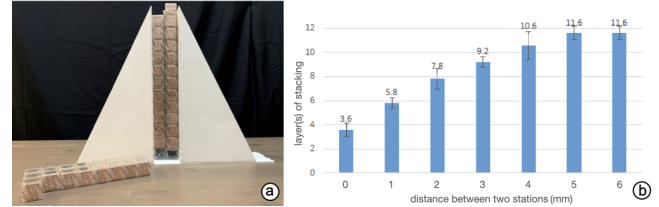


Figure 15: Station distance vs. brick stacking: (a) experiment apparatus; (b) results.

Using Bricks and Stations for 2.5D Construction. With a 1D or 2D array of stations, 1.5D or 2.5D rich-ID construction can be achieved with the bricks. Figure 16 shows our prototype system, which supports 1.5D or 2.5D rich-ID construction using 4 stations. Based on the experimental results, we increased the dimensions of brick from $30(W)\text{mm} \times 30(L)\text{mm}$ to $36(W)\text{mm} \times 36(L)\text{mm}$ by applying a 3mm-thick acrylic shell to each block, as shown in Figure 17a, and increases the dimension of station accordingly. The shelled blocks and stations keep the $d_{\text{station}} = 6\text{mm}$ yet they are still small enough to allow the users to grasp them between fingers. A 1-to-1 adapter (Figure 17b) can support the users to turn the top of each stack or station into a portal for sensing NFC-tagged tokens.

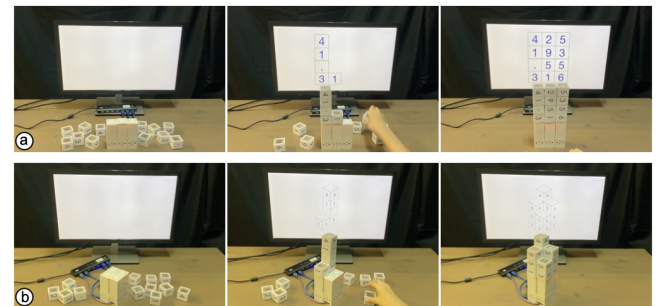


Figure 16: Constructions on tiled stations: (a) 1.5D construction on a 1×3 array of stations; (b) 2.5D construction on a 2×2 array of stations.

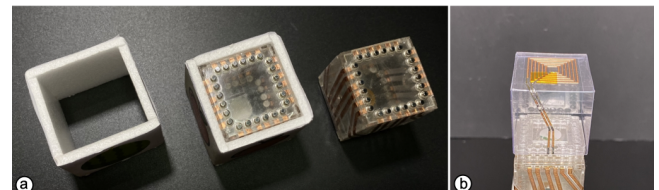


Figure 17: Hardware adaptation for tiling stations: (a) bricks with an additional shell that keeps the distance between blocks from the neighbor station; (b) 1-to-1 Adapter.

Identifying the Relative Position of Stations. Identifying the station's relative position allows for stacking the stations in another direction, and therefore supports batch operations by manipulating

the entire stack, as demonstrated in prior work [23]. To achieve the resolution of the stack’s relative position, we applied four additional pairs of NFC tags and antenna coil on the surface of each of the four sides of the stations, as shown in Figures 18 a and b. Each coil is connected to the multiplexer channel via transmission lines. Each tag is placed sufficiently far away from the coil next to it to make sure it cannot be detected accidentally. After one station connects to another, the two antenna coils placed at the two corresponding surface locations activate simultaneously and read the tag of each other. The two stations recognize the ID and face of the station so that the system can infer the topology based on the information.

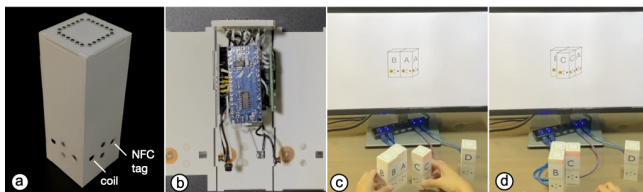


Figure 18: Tileable stations: (a) additional pairs of tag and coil are added on each side; (b) signal processing unit; (c-d) stacking stations side by side.

Supporting Effortless Tangible Interactions on 2.5D Constructions. Although the current 1-to-4 adapters and $N = 4$ blocks are still larger than the bricks, we make them compatible with the 2.5D system by simply thickening the shell of each brick and station to fit the size of blocks while considered $d_{station}$, as shown in Figure 10. With a larger (e.g., 3×5) grid of NFCStack stations deployed, the tangible Minecraft applications in RFIBricks [13] can be implemented in a much smaller form factor without depending on an external reader, supporting simultaneous interactions with multiple users, and allows for effortless inputs with the Blocks. Ultimately, we envision tangible interaction with the blocks on such a station can be as easy as throwing an inflatable dice.

7 DISCUSSION

Applications and Contribution. Many applications of Rich-ID building blocks have been proposed in the previous work, such as 3D modeling [1], physical computing [16], tangible programming (see the overview in [26]), gaming [23, 27], context construction [10, 23, 30], and so on. Education and entertainment also have been the main application domains of tangible user interfaces. Therefore, this paper does not aim at proposing new applications. Instead, we focus more on the technical contribution, which is the engineering and design of this building block design that enables novel capability – blending the effortless NFC-based tangible interaction into the passive rich-ID building block system. We highlight the use of the systems by showing simple examples and evaluating the performance of a system implementation to help future researchers build and extend their systems to the current results. Nonetheless, we are still interested in knowing how the next users will use the techniques and hardware platform to enrich and customize their applications. Therefore, running design workshops to collect more artifacts and design processes is considered an extension of this work.

Multiplexing vs. System performance. The multiplexer that we used in the station has a resistance of $\sim 70\Omega$, which lower our RLC circuit’s quality factor to $Q = 1.7$. Although a $Q \geq 1$ circuit is still compatible for near-field communication, the lossy RLC circuit did affect the performance of relay-based extension. In informal testing, we conducted the full-stack experiment with the relays in the same setting as Figure 12b and the same procedure as Section 5.2.1 to see how many relay connections allow a reader read a tag with and without the multiplexer. The results show that the tag can be read after 12 connections without the multiplexer, but only 7 connections can be made with the multiplexer. We suggest two solutions for future research. One is using multiple NFC reader IC instead of a multiplexed one so there is no additional resistance R_{mux} in the RLC circuit. Software-defined multiplexing, such as selecting only one NFC at a time using the SPI protocol, can be applied to avoid cross-talk. Another solution is using low-ohmic multiplexers to increase the RLC antenna’s Q factor.

More interactivity. Adding extra input and output modality to the NFCBricks system is more straightforward than previous work on the UHF RFID building blocks [23] or the NFC Stackers [35]. Some of the terminals can also be connected to the general-purpose input and output (GPIO) pins of the microcontroller directly so that the blocks can interface with more sensors (e.g., motion sensors), displays (e.g., OLED), and actuators (e.g., servo motors). These terminals can be added to the center of the blocks, so they do not necessarily compromise the stacking capability. Meanwhile, we suggest keeping these extra data and power lines properly away from the surface NFC antennas and transmission lines to not interfere with the stacking sensing and recognition.



Figure 19: Bricks made of printed circuit boards and pogo pins: (a) top view; (b) bottom view; (c) side view.

Durability and Scalability. Although the system supports personal fabrication, the durability, and scalability of the current proof-of-concept implementation are both limited as it is made of vinyl-cutting copper circuitry and plastic. Regarding electromechanical and mechanical durability, a semi-automated printed circuit board assembly (PCBA) and standard connectors should be considered. Figure 19 shows an example PCBA implementation of bricks, which is made of four pieces of PCB boards and standard POGO pins that can be reliably soldered on the PCB with improved durability of the system. We are also making blocks with flexible PCB to replace the current vinyl-cutting workflow. Regarding scalability, PCBA fabrication also reduced the manual assembly efforts and human errors and therefore ease the deployment at scale.

Being Water-proof and Dust-proof. NFC is occlusion-free and dust-proof. At the operating range of 13.56MHz, NFC is not significantly affected by water [8]. Therefore, if a station is sealed water-tight with an adapter mounted on the top, it can still detect a stack of blocks if each of them is also sealed water-tight. By mounting a magnet inside each block and adapter-mounted station, they can also support sturdy construction as bricks do. Although the size of the water-and-dust-proof NFCStack system will be larger than the one proposed in this paper because the size of the block depends on the size of the coils, it still has a high potential for making kids-friendly tangible kits that withstand unexpectedly creative use, especially when safety comes first.

8 CONCLUSION

We have presented NFCStack, a physical building blocks system that supports both stacking and interaction based on NFC. Based on the two antenna extension methods, we proposed three types of building blocks, brick, block, and adapter, that can handle concurrent stack events and blend physical construction and tangible interaction into a conventional NFC system. Evaluation results of a proof-of-concept implementation show that the system is effective. Generalizations of the NFCStack system are also presented with preliminary results. We sincerely hope future research can continue the investigation based on these results.

REFERENCES

- [1] David Anderson, James L. Frankel, Joe Marks, Darren Leigh, Eddie Sullivan, Jonathan Yedidia, and Kathy Ryall. 1999. Building Virtual Structures with Physical Blocks. In *Proceedings of the 12th Annual ACM Symposium on User Interface Software and Technology* (Asheville, North Carolina, USA) (*UIST '99*). ACM, New York, NY, USA, 71–72. <https://doi.org/10.1145/320719.322587>
- [2] Masahiro Ando, Yuichi Itoh, Toshiki Hosoi, Kazuki Takashima, Kosuke Nakajima, and Yoshifumi Kitamura. 2014. StackBlock: Block-shaped Interface for Flexible Stacking. In *Proceedings of the Adjunct Publication of the 27th Annual ACM Symposium on User Interface Software and Technology* (Honolulu, Hawaii, USA) (*UIST '14 Adjunct*). ACM, New York, NY, USA, 41–42. <https://doi.org/10.1145/2658779.2659104>
- [3] Daniel Avrahami and Scott E. Hudson. 2002. Forming Interactivity: A Tool for Rapid Prototyping of Physical Interactive Products. In *Proceedings of the 4th Conference on Designing Interactive Systems: Processes, Practices, Methods, and Techniques* (London, England) (*DIS '02*). Association for Computing Machinery, New York, NY, USA, 141–146. <https://doi.org/10.1145/778712.778735>
- [4] Maribeth Back, Jonathan Cohen, Rich Gold, Steve Harrison, and Scott Minneman. 2001. Listen Reader: An Electronically Augmented Paper-Based Book. In *Proceedings of the SIGCHI Conference on Human Factors in Computing Systems* (Seattle, Washington, USA) (*CHI '01*). Association for Computing Machinery, New York, NY, USA, 23–29. <https://doi.org/10.1145/365024.365031>
- [5] Tom Bartindale and Chris Harrison. 2009. Stacks on the Surface: Resolving Physical Order Using Fiducial Markers with Structured Transparency. In *Proceedings of the ACM International Conference on Interactive Tabletops and Surfaces* (Banff, Alberta, Canada) (*ITS '09*). ACM, New York, NY, USA, 57–60. <https://doi.org/10.1145/1731903.1731916>
- [6] Patrick Baudisch, Torsten Becker, and Frederik Rudeck. 2010. Lumino: Tangible Blocks for Tabletop Computers Based on Glass Fiber Bundles. In *ACM CHI 2010 Conference Proceedings* (Atlanta, Georgia, USA), 1165–1174.
- [7] Liwei Chan, Stefanie Müller, Anne Roudaut, and Patrick Baudisch. 2012. Cap-Stones and ZebraWidgets: Sensing Stacks of Building Blocks, Dials and Sliders on Capacitive Touch Screens. In *ACM CHI 2012 Conference Proceedings* (Austin, Texas, USA), 2189–2192.
- [8] Klaus Finkenzeller. 2003. *RFID Handbook: Fundamentals and Applications in Contactless Smart Cards and Identification* (2nd ed.). Wiley Publishing.
- [9] Audrey Girouard, Aneesh Tarun, and Roel Vertegaal. 2012. DisplayStacks: Interaction Techniques for Stacks of Flexible Thin-film Displays. In *Proceedings of the SIGCHI Conference on Human Factors in Computing Systems* (Austin, Texas, USA) (*CHI '12*). ACM, New York, NY, USA, 2431–2440. <https://doi.org/10.1145/2207676.2208406>
- [10] Alix Goguey, Cameron Steer, Andrés Lucero, Laurence Nigay, Deepak Ranjan Sahoo, Céline Coutrix, Anne Roudaut, Sriram Subramanian, Yutaka Tokuda, Timothy Neate, Jennifer Pearson, Simon Robinson, and Matt Jones. 2019. Pick-Cells: A Physically Reconfigurable Cell-composed Touchscreen. In *Proceedings of the 2019 CHI Conference on Human Factors in Computing Systems* (Glasgow, Scotland UK) (*CHI '19*). ACM, New York, NY, USA, Article 273, 14 pages. <https://doi.org/10.1145/3290605.3300503>
- [11] Jason T. Griffin, Steven Henry Fyke, Christopher Lyle Bender, Santiago Carbonell Duque, David Ryan Walker, and Jerome Pasquero. 2014. Near-field communication (NFC) system providing mobile wireless communications device operations based upon timing and sequence of NFC sensor communication and related methods. U.S. Patent 8,670,709.
- [12] Toshiki Hosoi, Kazuki Takashima, Tomoaki Adachi, Yuichi Itoh, and Yoshifumi Kitamura. 2014. A-blocks: Recognizing and Assessing Child Building Processes During Play with Toy Blocks. In *SIGGRAPH Asia 2014 Emerging Technologies* (Shenzhen, China) (*SA '14*). ACM, New York, NY, USA, Article 1, 2 pages. <https://doi.org/10.1145/2669047.2669061>
- [13] Meng-Ju Hsieh, Rong-Hao Liang, Da-Yuan Huang, Jheng-You Ke, and Bing-Yu Chen. 2018. RFIBricks: Interactive Building Blocks Based on RFID. In *Proceedings of the 2018 CHI Conference on Human Factors in Computing Systems* (Montreal QC, Canada) (*CHI '18*). Association for Computing Machinery, New York, NY, USA, 1–10. <https://doi.org/10.1145/3173574.3173763>
- [14] Hiroshi Ishii and Brygg Ullmer. 1997. Tangible Bits: Towards Seamless Interfaces Between People, Bits and Atoms. In *Proceedings of the ACM SIGCHI Conference on Human Factors in Computing Systems* (Atlanta, Georgia, USA) (*CHI '97*). ACM, New York, NY, USA, 234–241. <https://doi.org/10.1145/258549.258715>
- [15] Robert J.K. Jacob, Audrey Girouard, Leanne M. Hirshfield, Michael S. Horn, Orit Shaer, Erin Treacy Solovey, and Jamie Zigelbaum. 2008. Reality-Based Interaction: A Framework for Post-WIMP Interfaces. In *Proceedings of the SIGCHI Conference on Human Factors in Computing Systems* (Florence, Italy) (*CHI '08*). Association for Computing Machinery, New York, NY, USA, 201–210. <https://doi.org/10.1145/1357054.1357089>
- [16] Yoshifumi Kitamura, Yuichi Itoh, and Fumio Kishino. 2001. Real-Time 3D Interaction with ActiveCube. In *CHI '01 Extended Abstracts on Human Factors in Computing Systems* (Seattle, Washington) (*CHI EA '01*). Association for Computing Machinery, New York, NY, USA, 355–356. <https://doi.org/10.1145/634067.634277>
- [17] Jinha Lee, Yasuaki Kakehi, and Takeshi Naemura. 2009. Bloxels: Glowing Blocks as Volumetric Pixels. In *ACM SIGGRAPH 2009 Emerging Technologies* (New Orleans, Louisiana) (*SIGGRAPH '09*). Association for Computing Machinery, New York, NY, USA, Article 5, 1 pages. <https://doi.org/10.1145/1597956.1597961>
- [18] Jakob Leitner and Michael Haller. 2011. Geckos: Combining Magnets and Pressure Images to Enable New Tangible-object Design and Interaction. In *Proceedings of the SIGCHI Conference on Human Factors in Computing Systems* (Vancouver, BC, Canada) (*CHI '11*). ACM, New York, NY, USA, 2985–2994. <https://doi.org/10.1145/1978942.1979385>
- [19] Rong-Hao Liang, Liwei Chan, Hung-Yu Tseng, Han-Chih Kuo, Da-Yuan Huang, De-Nian Yang, and Bing-Yu Chen. 2014. GaussBricks: Magnetic Building Blocks for Constructive Tangible Interactions on Portable Displays. In *Proceedings of the SIGCHI Conference on Human Factors in Computing Systems* (Toronto, Ontario, Canada) (*CHI '14*). Association for Computing Machinery, New York, NY, USA, 3153–3162. <https://doi.org/10.1145/2556288.2557105>
- [20] Rong-Hao Liang and Zengrong Guo. 2021. NFCSense: Data-Defined Rich-ID Motion Sensing for Fluent Tangible Interaction Using a Commodity NFC Reader. Association for Computing Machinery, New York, NY, USA. <https://doi.org/10.1145/3411764.3445214>
- [21] Rong-Hao Liang, Meng-Ju Hsieh, Jheng-You Ke, Jr-Ling Guo, and Bing-Yu Chen. 2018. RFIMatch: Distributed Batteryless Near-Field Identification Using RFID-Tagged Magnet-Biased Reed Switches. In *Proceedings of the 31st Annual ACM Symposium on User Interface Software and Technology* (Berlin, Germany) (*UIST '18*). Association for Computing Machinery, New York, NY, USA, 473–483. <https://doi.org/10.1145/3242587.3242620>
- [22] Rong-Hao Liang, Han-Chih Kuo, Liwei Chan, De-Nian Yang, and Bing-Yu Chen. 2014. GaussStones: Shielded Magnetic Tangibles for Multi-Token Interactions on Portable Displays. In *Proceedings of the 27th Annual ACM Symposium on User Interface Software and Technology* (Honolulu, Hawaii, USA) (*UIST '14*). Association for Computing Machinery, New York, NY, USA, 365–372. <https://doi.org/10.1145/2642918.2647384>
- [23] Chin-Yuan Lu, Han-Wei Hsieh, Rong-Hao Liang, Chi-Jung Lee, Ling-Chien Yang, Mengru Xue, Jr-Ling Guo, Meng-Ju Hsieh, and Bing-Yu Chen. 2021. Combining Touchscreens with Passive Rich-ID Building Blocks to Support Context Construction in Touchscreen Interactions. Association for Computing Machinery, New York, NY, USA. <https://doi.org/10.1145/3411764.3445722>
- [24] Thomas W. Malone. 1983. How Do People Organize Their Desks?: Implications for the Design of Office Information Systems. *ACM Trans. Inf. Syst.* 1, 1 (Jan. 1983), 99–112. <https://doi.org/10.1145/357423.357430>
- [25] Einar Snee Martinussen and Timo Arnall. 2009. Designing with RFID. In *Proceedings of the 3rd International Conference on Tangible and Embedded Interaction* (Cambridge, United Kingdom) (*TEI '09*). Association for Computing Machinery, New York, NY, USA, 343–350. <https://doi.org/10.1145/1517664.1517734>

1045
1046
1047
1048
1049
1050
1051
1052
1053
1054
1055
1056
1057
1058
1059
1060
1061
1062
1063
1064
1065
1066
1067
1068
1069
1070
1071
1072
1073
1074
1075
1076
1077
1078
1079
1080
1081
1082
1083
1084
1085
1086
1087
1088
1089
1090
1091
1092
1093
1094
1095
1096
1097
1098
1099
1100
1101
1102
1103
1104
1105
1106
1107
1108
1109
1110
1111
1112
1113
1114
1115
1116
1117
1118
1119
1120
1121
1122
1123
1124
1125
1126
1127
1128
1129
1130
1131
1132
1133
1134
1135
1136
1137
1138
1139
1140
1141
1142
1143
1144
1145
1146
1147
1148
1149
1150
1151
1152
1153
1154
1155
1156
1157
1158
1159

- 1161 [26] Timothy S McNeaney. 2004. From turtles to Tangible Programming Bricks: 1219 explorations in physical language design. *Personal and Ubiquitous Computing* 8, 1220 5 (2004), 326–337.
- 1162 [27] David Merrill, Jeevan Kalanithi, and Pattie Maes. 2007. Siftables: Towards 1221 Sensor Network User Interfaces. In *Proceedings of the 1st International Conference on 1222 Tangible and Embedded Interaction* (Baton Rouge, Louisiana) (*TEI '07*). ACM, New 1223 York, NY, USA, 75–78. <https://doi.org/10.1145/1226969.1226984>
- 1163 [28] Farshid Salemi Parizi, Eric Whitmire, and Shwetak Patel. 2019. AuraRing: Precise 1224 Electromagnetic Finger Tracking. *Proc. ACM Interact. Mob. Wearable Ubiquitous 1225 Technol.* 3, 4, Article 150 (dec 2019), 28 pages. <https://doi.org/10.1145/3369831>
- 1164 [29] Amanda Parkes and Hiroshi Ishii. 2010. Bosu: <i>A Physical Programmable 1226 Design Tool for Transformability with Soft Mechanics</i>. In *Proceedings of 1227 the 8th ACM Conference on Designing Interactive Systems* (Aarhus, Denmark) 1228 (*DIS '10*). Association for Computing Machinery, New York, NY, USA, 189–198. 1229 <https://doi.org/10.1145/1858171.1858205>
- 1165 [30] Florian Perteneder, Kathrin Probst, Joanne Leong, Sebastian Gassler, Christian 1230 Rendl, Patrick Parzer, Katharina Fluch, Sophie Gahleitner, Sean Follmer, Hideki 1231 Koike, and Michael Haller. 2020. Foxels: Build Your Own Smart Furniture. In 1232 *Proceedings of the Fourteenth International Conference on Tangible, Embedded, 1233 and Embodied Interaction* (Sydney NSW, Australia) (*TEI '20*). Association for Computing 1234 Machinery, New York, NY, USA, 111–122. <https://doi.org/10.1145/3374920.3374935>
- 1166 [31] Hayes Solos Raffle, Amanda J. Parkes, and Hiroshi Ishii. 2004. *Topobo: A Con- 1235 structive Assembly System with Kinetic Memory*. Association for Computing 1236 Machinery, New York, NY, USA, 647–654. <https://doi.org/10.1145/985692.985774>
- 1167 [32] Jun Rekimoto, Brygg Ullmer, and Haruo Oba. 2001. DataTiles: A Modular 1237 Platform for Mixed Physical and Graphical Interactions. In *Proceedings of the SIGCHI 1238 Conference on Human Factors in Computing Systems* (Seattle, Washington, USA) 1239 (*CHI '01*). ACM, New York, NY, USA, 269–276. <https://doi.org/10.1145/365024.365115>
- 1168 [33] Ryo Takahashi, Masaaki Fukumoto, Changyo Han, Takuwa Sasatani, Yoshiaki 1240 Narusue, and Yoshihiro Kawahara. 2020. *TelemetRing: A Batteryless and Wire- 1241 less Ring-Shaped Keyboard Using Passive Inductive Telemetry*. Association for 1242 Computing Machinery, New York, NY, USA, 1161–1168. <https://doi.org/10.1145/3379337.3415873>
- 1169 [34] Brygg Ullmer, Hiroshi Ishii, and Robert J. K. Jacob. 2005. Token+constraint 1243 Systems for Tangible Interaction with Digital Information. *ACM Trans. Comput.-Hum. Interact.* 12, 1 (March 2005), 81–118. <https://doi.org/10.1145/1057237.1057242>
- 1170 [35] Nicolas Villar, Daniel Cletheroe, Greg Saul, Christian Holz, Tim Regan, Oscar 1244 Salandin, Misha Sra, Hui-Shyong Yeo, William Field, and Haiyan Zhang. 2018. Project 1245 Zanzibar: A Portable and Flexible Tangible Interaction Platform. In *Proceedings of the 1246 2018 CHI Conference on Human Factors in Computing Systems* (Montreal QC, Canada) 1247 (*CHI '18*). ACM, New York, NY, USA, Article 515, 13 pages. <https://doi.org/10.1145/3173574.3174089>
- 1171 [36] Oren Zuckerman, Saeed Arida, and Mitchel Resnick. 2005. Extending Tangible 1248 Interfaces for Education: Digital Montessori-Inspired Manipulatives. *CHI 2005: 1249 Technology, Safety, Community: Conference Proceedings - Conference on Human 1250 Factors in Computing Systems*. <https://doi.org/10.1145/1054972.1055093>
- 1172
1173
1174
1175
1176
1177
1178
1179
1180
1181
1182
1183
1184
1185
1186
1187
1188
1189
1190
1191
1192
1193
1194
1195
1196
1197
1198
1199
1200
1201
1202
1203
1204
1205
1206
1207
1208
1209
1210
1211
1212
1213
1214
1215
1216
1217
1218